Automatic control-line flight for high altitude wind energy drones

Antonello Cherubini, Balazs Szalai, Roland Schmehl, Marco Fontana
Sant'Anna University, Enevate B.V., TU Delft, University of Trento
a.cherubini@santannapisa.it

Abstract

Airborne Wind Energy Systems can extract renewable energy from winds at higher altitudes than conventional wind turbines. However, their maximum altitude is relatively low, especially if compared to several thousand meters where several kW per square meter are available. The reason for this can be identified in the aerodynamic drag of the cable.

The dual wind drone concept aims at reducing significantly the aerodynamic drag of the cable, thus potentially allowing to reach higher altitudes, with the final goal of building a wind generator that either has a lower cost or generates more power. However, to successfully deploy a dual wind drone system, several challenges must be met, such as autonomous take-off and landing, steady state stability, and demonstration of power generation.

In order to assess the viability of autonomous take-off and landing of a dual wind drone system, this poster presents the results of a test campaign that demonstrates full autonomous take-off and landing capabilities of a small scale single wind drone flying round the pole in an axisymmetric configuration. The poster first introduces a dynamic model for the drone and then describes a test bench composed by a small scale model plane and a ground station provided with sensors. The experimental results are given.

The passive stability of the flight of the single wind drone suggests that autonomous take-off and landing of a dual wind drone system can be easily achieved.

Introduction

Despite being capable of reaching higher altitudes with respect to conventional wind turbines, AWES are currently limited to a maximum altitude of several hundred meters, a relatively low altitude if compared to several thousand meters where the power carried by the wind is substantially higher [1]. In order to understand the main physical reason for this limitation, two effects should be considered. First, an increase in altitude corresponds to an availability of more powerful winds [2, 3] and, second, an increase in altitude comes from an increase in tether length, and this causes in turn an increase in energy dissipation through the cable aerodynamic drag. For real-world wind profiles and tether dimensions, it is easy to show that, when attempting to increase the altitude, the power that would be lost through the cable drag is more than the power that would be gained because of the higher energy availability [4, 5].

In order to overcome this limitation and build a generator finally able to reach higher altitudes, a dual wind drone concept was first patented in 1976 [6] and then investigated in [7, 8, 9, 10, 11, 12]. The physical advantage of a dual wind drone arrangement is summarized in Fig. 1. By having a shared cable that is kept fixed by the controller, a dual (or multiple) wind drone system would be able to increase the operating altitude without increasing the energy dissipated by the cable aerodynamic drag (see Fig. 1-right). This would potentially allow the drones to reach higher altitudes, thus accessing more powerful winds, thereby generating a larger amount of power.

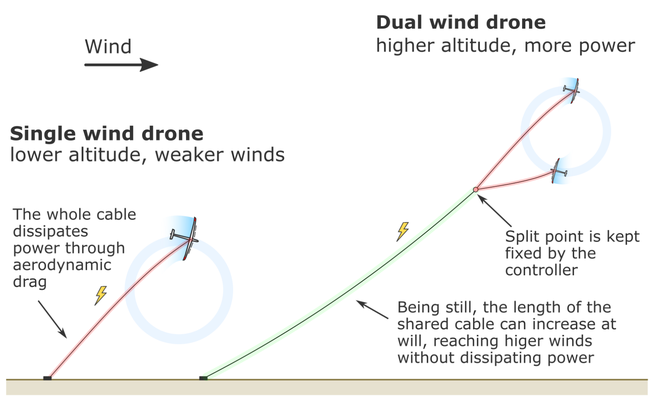

Figure 1: The advantage of a dual wind drone system. In a single wind drone (left) the whole cable (red) dissipates power through aerodynamic drag. For this reason the optimal flight altitude for single wind drones is relatively low. In a dual wind drone arrangement (right) only the top moving cables (red) dissipate power.

Dynamic model of take off and landing of a single drone

The following forces are considered in the force balance: tether tension $\boldsymbol{T}$, motor thrust $\boldsymbol{F_m}$, lift $\boldsymbol{L}$ and drag $\boldsymbol{D}$ of the main wing, lift of the elevator $\boldsymbol{L_e}$, and gravity force $\boldsymbol{F_g}$. With reference to Fig. 2, the vector expressions in the drone reference system can be written as:

$$\begin{aligned}
\boldsymbol{T} &= -T\,\hat{\boldsymbol{e}}_{\boldsymbol{pitch}} \\
\boldsymbol{F_m} &= F_m\,\hat{\boldsymbol{e}}_{\boldsymbol{roll}} \\
\boldsymbol{L} &= -L\cos\alpha\,\hat{\boldsymbol{e}}_{\boldsymbol{yaw}} + L\sin\alpha\,\hat{\boldsymbol{e}}_{\boldsymbol{roll}} \\
\boldsymbol{L_e} &= -L_e\cos\alpha_e\,\hat{\boldsymbol{e}}_{\boldsymbol{yaw}} + L_e\sin\alpha_e\,\hat{\boldsymbol{e}}_{\boldsymbol{roll}} \\
\boldsymbol{D} &= -D\sin\alpha\,\hat{\boldsymbol{e}}_{\boldsymbol{yaw}} - D\cos\alpha\,\hat{\boldsymbol{e}}_{\boldsymbol{roll}} \\
\boldsymbol{F_g} &= (mg\sin\theta\cos\psi)\,\hat{\boldsymbol{e}}_{\boldsymbol{yaw}} - (mg\sin\theta\sin\psi)\,\hat{\boldsymbol{e}}_{\boldsymbol{roll}} + \\
&\quad - (mg\cos\theta)\,\hat{\boldsymbol{e}}_{\boldsymbol{pitch}}
\end{aligned} \tag{1}$$

where α is the angle of attack, T, F_m, L, L_e, D, F_g are the magnitudes of the forces.

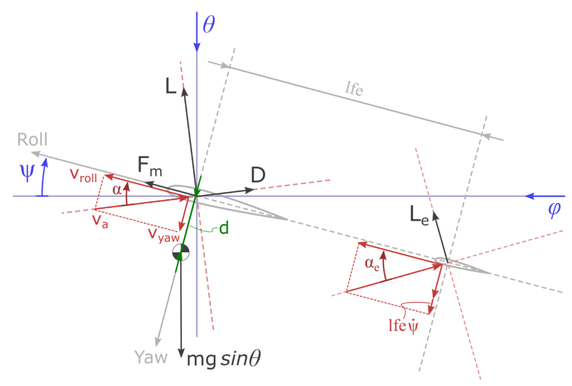

Figure 2: Force balance at the wind drone. View along the tether direction. The balance lies on the θ-φ plane. The forces are shown in black. The roll and yaw axes of the drone reference system are shown in grey. The velocity triangles are shown in red.

$$\begin{aligned}
a_{roll} &= \frac{1}{m}\left(F_m + L\sin\alpha - D\cos\alpha + L_e\sin\alpha_e - mg\sin\theta\sin\psi\right) \\
a_{yaw} &= \frac{1}{m}\left(-L\cos\alpha - D\sin\alpha - L_e\cos\alpha_e + mg\sin\theta\cos\psi\right)
\end{aligned} \tag{2}$$

and, from the force balance along the pitch axis, the tether force expression results in

$$T = m\left(r\dot{\theta}^2 + r\dot{\varphi}^2\sin^2\theta - g\cos\theta\right) \tag{3}$$

$$\begin{aligned}
J\ddot{\psi} &= +M_e + M_g \\
M_e &= -l_{fe}\,L_e\cos\alpha_e \\
M_g &= -mg\,d\sin\psi
\end{aligned} \tag{4}$$

notice that the airflow velocity at the elevator is assumed equal to the airflow velocity at the main wing for the sake of simplicity, while the angle of attack of the elevator is considered different to take into account the natural stabilization of the pitch motion.

Stability

Some important information about the altitude stability of control line flight can be easily understood from the horizontal steady-state case, i.e. when the drone is flying at a constant flight velocity. In particular the flight is stable in altitude when $\theta > 90\ deg$ (drone below the horizontal plane that passes through the ground attachment point of the tether) but it is unstable when $\theta < 90\ deg$ (drone above the ground station, towards the zenith). This can be explained by perturbing the vertical force equilibrium of the steady-state case.

Automatic flight

A picture of the overall setup is shown in Fig. 3.

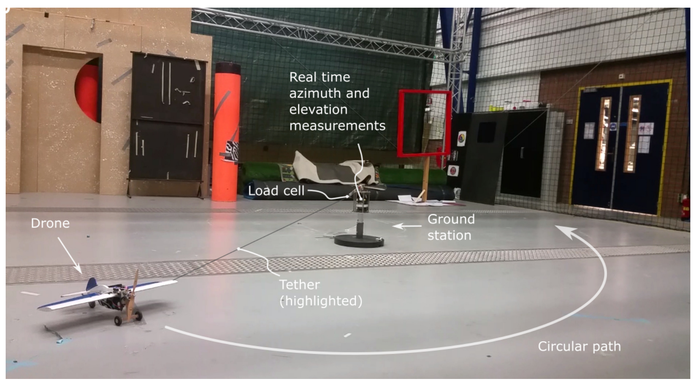

Figure 3: The automatic model ready to fly at the Cyber-Zoo facility of TU Delft.

A fully automatic 'take off - fly - land' sequence can be achieved by using the test setup introduced in Fig 3.

Fig. 4 shows the time history of two consecutive sequences performed in laboratory environment (without wind) with a simple feed-forward controller (a video is available in [13]).

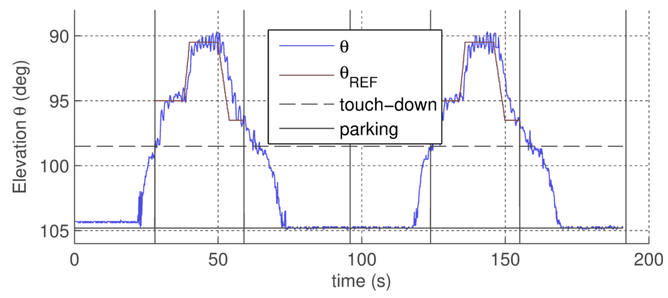

Figure 4: Automatic flight. The charts show the results from two consecutive automatic 'take off - fly - land' sequences. In each sequence, take off is performed first, then the drone tracks elevation angles θ of 95, 90.5 and 96.5 degrees and then the drone lands. The chart shows throttle command (top), nose-up command (middle) and elevation angle (bottom).

Considering the simple feed-forward controller, the overall automatic sequence is remarkably repeatable.

Conclusions

In this work the take off and landing for the dancing drone concept has been investigated by means of a rotating drone in axisymmetrical configuration following the example of control line flight. A dynamic model has been developed and an experimental test campaign has been carried out. Full automatic take-off and landing capabilities were experimentally demonstrated and two sample 'take off - fly - land' sequences are reported. Given the flight stability and the repeatability of the sequences, the dual wind drone system is foreseen to have autonomous take-off and landing capabilities and further research in this direction is highly encouraged.

References

[1] Antonello Cherubini, Andrea Papini, Rocco Vertechy, and Marco Fontana. Airborne wind energy systems: A review of the technologies.

[2] Cristina L. Archer and Ken Caldeira. Global Assessment of High-Altitude Wind Power.

[3] Cristina Archer and Ken Caldeira. Atlas of high altitude wind power.

[4] Antonello Cherubini and Marco Fontana. Assessment of Megawatt-Scale Wind Energy Drone Generators at Jet Stream Altitude.

[5] Antonello Cherubini. Kite Dynamics and Wind Energy Harvesting.

[6] Peter R. Payne. Self erecting windmill. *US patent*.

[7] Mario Zanon, Sébastien Gros, Joel Andersson, and Moritz Diehl. Airborne Wind Energy Based on Dual Airfoils.

[8] Mario Zanon, Sebastien Gros, Johan Meyers, and Moritz Diehl. Airborne Wind Energy: Airfoil-Airmass Interaction.

[9] Mario Zanon, Sébastien Gros, Joel Andersson, and Moritz Diehl. Airborne wind energy based on dual airfoils.

[10] S. Gros and M. Diehl. Modeling of airborne wind energy systems in natural coordinates. In U. Ahrens, M. Diehl, and R. Schmehl, editors, *Airborne Wind Energy*.

[11] M. Diehl, G. Horn, and M. Zanon. Multiple wing systems - an alternative to upscaling?

[12] Moritz Diehl. Basic Concepts and Physical Foundations. *Airborne Wind Energy, U. Ahrens, M. Diehl, R. Schmehl Eds.*

[13] *Video url: youtube.com/watch?v=PaeCZ72ghRQ (2016)*, 2016.

Acknowledgements

This work was carried out with funds from Scuola Superiore Sant'Anna and Delft University of Technology